JOURNAL OF GEOPHYSICAL RESEARCH, VOL. 106, NO. A4, PAGES 5693–5708, APRIL 1, 2001

Helium energetics in the high-latitude solar wind: Ulysses observations

D. B. Reisenfeld, S. P. Gary, J. T. Gosling, and J. T. Steinberg

Los Alamos National Laboratory, Los Alamos, New Mexico

D. J. McComas

Southwest Research Institute, San Antonio, Texas

B. E. Goldstein and M. Neugebauer

Jet Propulsion Laboratory, Pasadena, California

Abstract. We present a study of the interplanetary evolution of solar wind helium (alpha particle) energetics. The analysis of Ulysses observations of the fast high-latitude solar wind concentrates on the radial evolution of the alpha-proton differential streaming $v_{\alpha p}$, the alpha temperature, and the alpha temperature anisotropy. Ulysses observations show that the average $v_{\alpha p}$ steadily decreases with radius, ranging from $\sim$40 km s^{-1} at 1.5 AU to $\sim$15 km s^{-1} at 4.2 AU. In addition, observations indicate that the alphas cool more slowly than what would be expected from adiabatic expansion. The radial increase in the nonadiabatic heat content of the alphas matches the free energy liberated as $v_{\alpha p}$ decreases with distance, suggesting that the dissipated energy acts to heat the alpha particles. The alphas also exhibit a temperature anisotropy of $T_{\perp\alpha}/T_{\|\alpha} = 0.87$, which is essentially constant with distance. These and other observations reported here place stringent constraints on recent plasma microinstability models that attempt to explain the evolution of alpha-proton differential streaming and ion heating in the heliosphere.

1. Introduction

Solar wind helium ions have been the subject of extensive study because they serve as invaluable tools for probing the nature of the solar wind. In particular, those properties of helium ions that distinguish them from the more abundant protons can help us understand the mechanisms of solar wind acceleration and the subsequent evolution of interplanetary solar wind flow. The two principal kinematic properties that distinguish helium ions from protons are (1) helium ions drift faster than the protons along the magnetic field at relative speeds from a few to 50 km s^{-1} at 1 AU, and (2) helium ions are, on average, significantly hotter than protons, typically by a factor of 4-5 at 1 AU.

The differential streaming between the alphas and the protons has been a subject of particular interest. This phenomenon was first observed by *Robbins et al.* [1970]. Helios in-ecliptic observations between 0.3 and 1.0 AU show that near the Sun the alpha-proton differential speed $v_{\alpha p}$ is as high as 150 km s^{-1} and that it slows as the solar wind propagates outward [*Marsch et al.*, 1982a]. The $v_{\alpha p}$ also tends to scale with the proton speed v_p. In fast streams, $v_{\alpha p}$ approaches the local Alfvén speed v_A whereas in slow plasma, $v_{\alpha p}$ is much less, only a few kiometers per second. On average, $v_{\alpha p} \sim 0$ km s^{-1} at the heliospheric current sheet [*Borrini et al.*, 1981]. At greater heliocentric distances these trends persist. Ulysses observations at both high and low latitudes and at distances between 1 and 5.4 AU show that $v_{\alpha p}$ continues to slow with increasing distance, dropping well below v_A even in high-speed flow [*Neugebauer et al.*, 1996].

Although considerable data have been collected that well characterize the differential streaming, the cause for the initial superacceleration of the alphas and their subsequent deceleration relative to the protons is not well understood. Regarding the initial helium acceleration, recent findings from the Ultraviolet Coronograph Spectrometer (UVCS) instrument aboard the SOHO spacecraft [*Kohl et al.*, 1998] support a model for the preferential heating and acceleration of heavy ions through ion cyclotron resonance heating [*Hollweg and Turner*, 1978; *Axford et al.*, 1999; *Cranmer et al.*, 1999]. This model explains the observed perpendicular heating of oxygen ions to temperatures $\sim$60 times the proton temperature and the subsequent superaccel-

Paper number 2000JA000317.
0148-0227/01/2000JA000317$09.00

eration of oxygen. This same model predicts preferential heating and acceleration of helium ions; however, because the UVCS instrument was not designed to observe helium, it has yet to be verified.

The apparent association of $v_{\alpha p}$ with the Alfvén speed in the solar wind and the observed gradual decrease of $v_{\alpha p}/v_A$ with distance from the Sun suggest that some mechanism acts to constrain the alpha/proton relative drift speed. *Marsch and Livi* [1987] showed that alpha particles usually damp the proton/proton magnetosonic instability, but it is not clear whether such damping acts to speed up or slow down the alphas. Here we suggest (see also *Gary et al.* [2000b]) that instabilities driven by the alpha/proton relative drift may constrain $v_{\alpha p}$ to the order of v_A.

Coulomb collisions have also been suggested as a possible mechanism for slowing the alphas, but *Neugebauer et al.* [1996] show the collision times are too great for this to be an effective mechanism, except perhaps in the slow, dense flow near the heliomagnetic current sheet. Finally, "rotational" forces on the alphas as they flow relative to the protons along the spiraling magnetic field have also been considered [*McKenzie et al.*, 1979; *Hollweg and Isenberg,* 1981; *Mckenzie and Axford,* 1983]. However, *Neugebauer et al.* [1996] show that there is no dependence of $v_{\alpha p}$ on solar latitude, which would be expected if rotational forces were significant. Thus they conclude that such forces play no significant role in the deceleration of the alphas. We will return to this issue in the discussion of the helium energetics (section 3.3).

It is well established by the great number of plasma experiments flown at 1 AU that solar wind helium and hydrogen are most often far from being in thermodynamic equilibrium. Taking values compiled from the IMP 6, 7 and 8 spacecraft [*Feldman et al.*, 1977], which are typical of the values observed by other spacecraft, at 1 AU the helium temperature is, on average, 5.8×10^5 K compared to the average proton temperature of 1.2×10^5 K. The reported average alpha-proton temperature ratio, T_α/T_p, is 4.9 ± 1.8. The temperature ratio is also velocity dependent: in low-speed flow ($v_p < 350$ km s^{-1}), $T_\alpha/T_p = 3.2 \pm 0.9$, whereas in high-speed flow ($v_p > 650$ km s^{-1}), $T_\alpha/T_p = 6.2 \pm 1.3$.

The radial dependence of T_α/T_p and of the alpha temperature was investigated by the Helios spacecraft, but with perhaps contradictory results. The temperature ratio based on single-spacecraft observations appears to drop with heliocentric distance [*Marsch et al.*, 1982a]. For flow above 600 km s^{-1} the ratio varies from 4.5 at 0.3 AU to 3.0 at 1 AU, and for flow below 400 km s^{-1} the ratio falls from 2.9 at 0.3 AU to 2.3 at 1 AU. The variation with distance is also reported in terms of a radial temperature gradient: in high-speed flow the parallel alpha temperature $T_{\|\alpha}$ goes as $r^{-1.15}$, but in the slow wind the gradient is flatter: $T_{\|\alpha} \sim r^{-0.75}$. However, the reported temperature ratios as observed when Helios 1 and 2 were radially aligned show the opposite trend, namely, an increasing temperature ratio with distance [*Schwenn et al.*, 1981]. The calculated alpha radial temperature gradient based on these data is much flatter: $T_{\|\alpha} \sim r^{-0.35}$. This latter observation, however, is based on a fairly sparse set of temperature observations; thus it is arguable that this is not typical of the solar wind. Note also that all the Helios temperature ratios reported at 1 AU are significantly below those reported by the IMP spacecraft.

One important aspect of the Helios observations that is consistent in all cases is that the radial decrease in the alpha temperature is shallower than $r^{-4/3}$, the expected falloff for pure adiabatic expansion in an isotropic plasma. This is an indication of heating of alpha particles between 0.3 and 1 AU.

For completeness we note that the same phenomena associated with helium appear to act on all solar wind heavy ions [see, e.g., *von Steiger et al.*, 1995, *Hefti et al.*, 1998, and references therein]. All heavy ions tend to drift faster than the protons at speeds comparable to $v_{\alpha p}$. Additionally, they are most often hotter than protons. The temperature ratios among the heavy ions (including helium) scale closely with ion mass; however, as with helium, the ion temperatures relative to hydrogen are not mass proportional. Rather, they show the same proton-speed dependence as helium.

In this report we focus on the interplanetary evolution of solar wind helium ion energetics as observed at high latitudes by Ulysses during its first orbit. After some introductory comments on the instrumentation and analysis procedure (section 2), we present observations of high-speed solar wind flow concentrating on the radial evolution of the helium ion temperature (section 3.1), temperature anisotropy (section 3.2), energetics(section 3.3) and differential streaming (section 3.4). In section 4 we argue that these parameters are related and that the observational data presented here place more stringent constraints on theoretical models that attempt to explain the evolution of alpha-proton differential streaming and ion heating in the heliosphere.

2. Instrumentation and Observational Considerations

This study is based on Ulysses solar wind plasma observations from the Los Alamos solar wind ion spectrometer [*Bame et al.*, 1992] and magnetic field observations from the Imperial College/Jet Propulsion Laboratory (JPL) magnetometer [*Balogh et al.*, 1992]. The data presented here were collected between May 1995 and December 1996 when Ulysses was traveling on the outbound leg of its first polar orbit and was immersed in continuous high-speed flow at latitudes above 30° N. This corresponds to radial distances between 1.5 and 4.2 AU. During this period the spacecraft instruments detected no coronal mass ejections (CMEs), shocks, or major compression waves. Thus we have a data set very useful for the study of solar wind microphysics. There is minimal processing of the plasma by macroscopic events

that can easily overwhelm the trends we seek to investigate. The data set is limited to distances within 4.2 AU because soon after Ulysses passed beyond this point, it began intersecting stream interaction regions [*Gosling,* 1996] where the plasma properties began to deviate significantly from the steady flow intended for this study.

Plasma moments (densities, velocities, temperatures) for protons and alpha particles have been calculated separately by integration of the particle distribution functions. The analysis makes use of measurements taken at the highest resolution, typically 4 min. Plasma properties requiring the evaluation of the distribution profile transverse to the radial (antisunward) direction require special consideration. The Ulysses ion spectrometer has a 5° polar angular resolution, which makes it difficult to calculate accurate temperature and velocity components perpendicular to the radial direction. This is particularly true for high solar wind speeds and at large heliocentric distances where the solar wind is cold. In such cases the value of the distribution function can drop by many orders of magnitude between adjacent angular measurements, making it impossible to determine the transverse temperature or velocity with any reasonable accuracy. On the other hand, the instrument energy/charge resolution is very good (5%), enabling quite accurate radial velocity and temperature measurements.

Of particular relevance here is the alpha-proton streaming velocity $v_{\alpha p}$, which can have a significant transverse component. To overcome the difficulties described above, we take advantage of the fact that the alphas stream relative to the protons along the magnetic field [e.g., *Asbridge et al.,* 1976; *Marsch et al.,* 1982a; *Steinberg et al.,* 1996]. Thus we calculate $v_{\alpha p}$ as follows:

$$v_{\alpha p} = \frac{v_{r\alpha} - v_{rp}}{\cos\theta_B}, \tag{1}$$

where $v_{r\alpha}$ and v_{rp} are the radial velocity components of the alpha particles and protons, respectively, and θ_B is the measured instantaneous angle between the magnetic field and the antisunward radial vector. When calculating $v_{\alpha p}$, we only include observations where $\cos\theta_B \geq 0.3$ ($\theta_B \leq 72.5°$). For values less than this the radial difference becomes subject to significant measurement uncertainty and is not a reliable proxy for the full vector difference.

The second parameter necessary for this study that depends on a measurement of the transverse distribution function is the alpha temperature anisotropy. Discussion of how we handle this measurement difficulty will be deferred to section 3.2.

3. Observations

3.1. Temperature Evolution

Figure 1 displays the alpha-proton temperature ratio as a function of heliocentric radial distance. Each data point represents the median temperature ratio for a 10-day interval. The thick bars span the 25% to 75% range of the distribution, and the thin bars span the 5% to 95% range. Binning was performed over 10-day intervals (~0.4 solar rotations) because at finer resolution, clarity of the plot degrades, yet the resolution is still fine enough that evolutionary trends are discernible over relatively short distances. The temperatures were calculated from the one-dimensional distribution func-

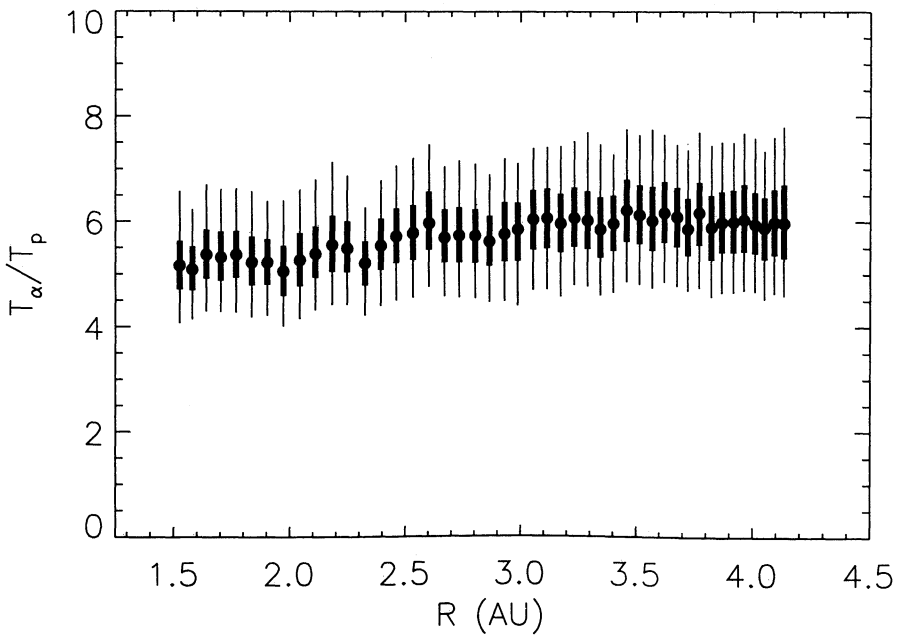

Figure 1. Alpha-proton temperature ratio as a function of heliocentric distance. Each data point represents the median temperature ratio over 10-day bins. The thin bars span the 5-95% percentiles, and the thick bars span the 25-75% percentiles.

tion (the three-dimensional distribution summed over angle).

The average temperature ratio at 1.5 AU is 5.1 and slowly increases to 6.0 at 3 AU, after which it remains relatively flat. The gradient of the temperature ratio follows an $r^{0.2}$ power law and shows negligible latitudinal variation, consistent with the detailed analysis of the radial and latitudinal dependencies of solar wind properties performed by *McComas et al.* [2000]. Extrapolating the temperature ratio back to 1 AU results in a value of 5.0. This value is ~20% lower than the T_α/T_p ratio reported by *Feldman et al.* [1977] for ecliptic high-speed flow, but it is within their quoted uncertainty of ±25%. On the other hand, the extrapolated 1 AU value is significantly higher than the quoted Helios 1.0 AU value of $T_\alpha/T_p = 3$.

The implication of the growing temperature ratio with radius is that the alphas cool less rapidly than the protons as the solar wind expands. This fact is quantified in greater detail in Figure 2, which plots the (log) helium temperature as a function of (log) helium density.

Here, $\log T_\alpha$ and $\log N_\alpha$ roughly follow a linear relation which can be expressed by a single polytrope relation of the form $T = aN^{\gamma-1}$, where γ is the polytropic exponent, which in this case has a value of 1.40. Polytrope relations are often used to describe the evolution of the internal energy of a gas in the absence of an explicit energy equation. In a strict interpretation, polytrope relations should only be applied when following the evolution of a single parcel of plasma [*Gosling,* 1999; *Skoug et al.,* 2000]. However, in the uniform, high-latitude flow under consideration here, we make the reasonable assumption that although we are not following individual parcels, their average behavior is consistent. Thus as we follow the radial evolution of the solar wind as a whole, this serves as a proxy for following the radial evolution of a typical individual parcel.

For an ideal isotropic gas, $\gamma = 1$ for the case of isothermal expansion and $\gamma = 5/3$, the ratio of specific heats, for the case of adiabatic expansion. Thus the observed value of $\gamma = 1.40$ for the alpha particles implies nonadiabatic expansion, and the fact that they follow a single polytrope relation implies the presence of a nearly continuous, uniform heat input as they expand. By comparison, it was shown by *Feldman et al.* [1998] for the same data set as used here that the protons follow a single polytrope relation with $\gamma = 1.51$. This value is closer to the adiabatic value but is slightly lower, also indicating a weak, continuous heat input into the protons as they expand.

Another way to express the presence of heating is to look at the radial temperature gradient. For the alphas, $T_\alpha \propto r^{-0.8}$, and for the protons, $T_p \propto r^{-1.0}$. By contrast, the expected radial falloff for adiabatic expansion is $r^{-4/3}$ (assuming $N \propto r^{-2}$ and an isotropic plasma; see next section for consequences when the assumption of isotropy is lifted). Note also that the observed T_α gradient falls between the gradients of $r^{-1.15}$ and $r^{-0.75}$ derived from Helios single-spacecraft observations of high- and low-speed wind, respectively [*Marsch et al.*, 1982a]. We would expect that the Helios high-speed T_α gradient should be the more appropriate for comparison to the Ulysses T_α gradient; however, these do not agree very

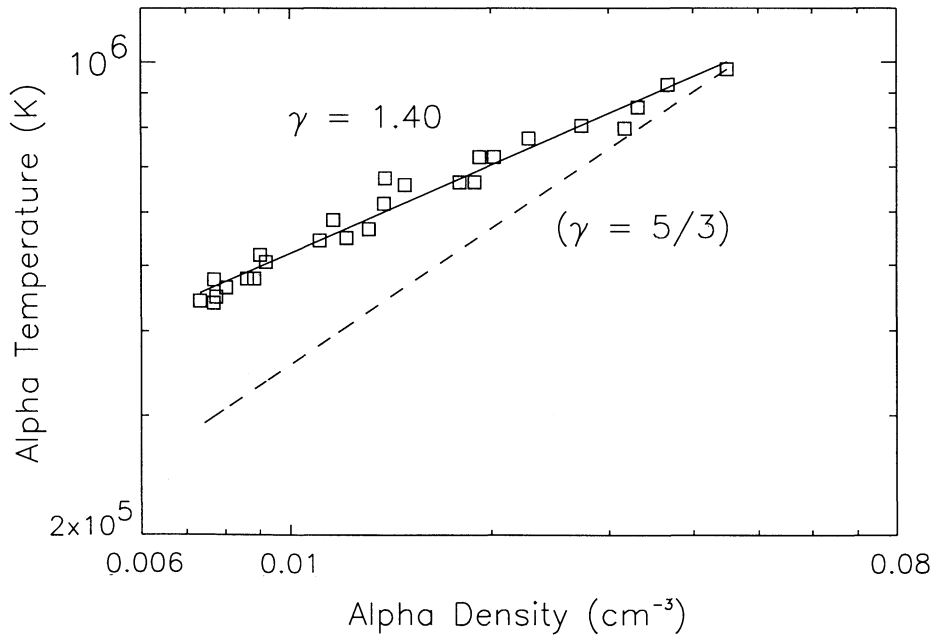

Figure 2. The relation between alpha temperature T_α and alpha density n_α, showing the existence of a single polytrope relation for the radial evolution of the alpha temperature. The slope of the line, 0.40, corresponds to a polytropic exponent of $\gamma \sim 1.40$. Each point represents the mean temperature and density for 0.05 AU radial bins.

well. This may suggest that at high latitudes a different mechanism is at work to govern the helium energetics than in the ecliptic.

3.2. Temperature Anisotropy

At distances beyond a few tenths of an AU the ion component of the solar wind is essentially collision less, particularly in high-speed flow. At 1 AU the proton-proton and alpha-proton collision times are of the order of 10 times the solar wind expansion time [*Feldman et al.*, 1977]. Consequently, it is not expected that the alpha distribution function should be isotropic. In fact, in the complete absence of coupling between the parallel and perpendicular temperatures (with respect to the local magnetic field direction), the two components should diverge rapidly, governed by the double adiabatic invariants [*Chew et al.*, 1956],

$$\frac{d}{dt}\left(\frac{T_{\|}B^2}{n^2}\right) = 0 \quad (2)$$

$$\frac{d}{dt}\left(\frac{T_{\perp}}{B}\right) = 0, \quad (3)$$

where $T_{\|}$ and $T_{\perp}$ are temperatures parallel and perpendicular to the local magnetic field $\mathbf{B}$, respectively; n is the number density, and d/dt is the convective derivative $\partial/\partial t + \mathbf{v}\cdot\nabla$. For a purely radial field, $B \sim r^{-2}$ and, consequently, $T_{\|}$ would remain constant while $T_{\perp}$ would fall as r^{-2}. In the more realistic case of B following a Parker spiral structure, $T_{\|}$ will no longer be constant but will fall with radius, and $T_{\perp}$ will not fall quite as rapidly. Nevertheless, they will still remain quite different: for 400 km s^{-1} flow, $T_{\perp}/T_{\|} = 1/32$ at 1 AU [see, e.g., *Phillips and Gosling*, 1990]. Nothing close to such a large anisotropy has ever been observed in the solar wind, with the implication that a mechanism other than Coulomb collisions must act to couple the temperature components. A likely alternative is some sort of wave-particle interaction as has been suggested by a number of authors [*Marsch et al.*, 1982b; *Meister*, 1992; *Kellogg*, 2000; *Gary et al.*, 2000a].

As discussed in section 2, the measurement accuracy of the transverse component of the ion distribution function is poor owing to the combination of high-speed solar wind and the large distance of Ulysses from the Sun. Thus we must rely on 1-D measurements of the distribution function along the energy axis to evaluate the temperature anisotropy. Of course, we cannot determine the instantaneous temperature anisotropy, but we can take advantage of (noncompressive) fluctuations in the magnetic field direction over the course of some hours to determine an "average" anisotropy for this interval.

We proceed as follows: at the high latitudes considered here, the solar wind flow is almost always within 1° of the radial (antisunward) direction. Thus since the velocity (energy flux) vector is essentially parallel to the radial direction, the 1-D temperature moment along the energy/charge axis is effectively a temperature measurement parallel to the radial direction. Thus, when the magnetic field is radial, the 1-D radial temperature measurement is a measure of $T_{\|}$. When B is transverse, the 1-D radial temperature is a measure of $T_{\perp}$. Therefore, to determine the helium temperature anisotropy, we compare radial temperatures when B is radial to times when B is transverse.

For this method to work, we must select time intervals short enough that the temperature distribution does not evolve significantly and also times when the changes in the field direction are not associated with dynamic changes in the plasma. Fortunately, such times are common in the solar wind, particularly at high latitudes, because of the near-ubiquitous presence of large-amplitude Alfvén waves. *Smith et al.* [1995] report that Alfvén waves are almost continuously present at high latitudes and at small heliospheric distances, slowly diminishing in frequency of occurrence with distance, but prevalent even out to 4 AU. Because the field fluctuations associated with Alfvén waves are largely noncompressive swings in the field direction, changes in the radial temperature as the field changes direction indicate a temperature anisotropy. Figure 3 shows solar wind parameters for a typical high-latitude 16-hour interval. The first two panels show the N-S magnetic field component B_N and velocity component v_N, which demonstrate that the field fluctuations are indeed Alfvénic. The magnetic field direction and the 1-D alpha temperature are compared in the third and fourth panels. The (anti)correlated variation of the magnetic field direction and temperature demonstrate the presence of the temperature anisotropy. The fifth panel of Figure 3 shows a scatterplot of θ_B versus T_{α} to make the correlation more apparent. Over this interval the anisotropy is significant, $T_{\perp\alpha}/T_{\|\alpha} = 0.7$.

Figure 4 shows the observed temperature anisotropy for helium versus heliocentric distance, indicating an average anisotropy of $T_{\perp\alpha}/T_{\|\alpha} = 0.87 \pm 0.092$ (at 1σ) that is essentially independent of distance. Each point represents a calculation of the temperature anisotropy using the prescription described above for a 12-hour period when Alfvén waves were continuously present. Interval selection was performed by calculating the correlation between B_N and v_N. Twelve-hour periods for which the correlation coefficient between B_N and v_N was >0.85 were included. We should point out that the observed anisotropy is not particularly sensitive to the choice of correlation criteria or correlation interval, which is a reflection of the fact that the high-latitude solar wind is essentially unstructured and that fluctuations in the field direction are almost always due to Alfvén waves. The ± 0.092 scatter in the observed anisotropy values reflects actual fluctuations of the temperature anisotropy. The instrumental uncertainty in determining the temperature ratio is negligible.

The mean anisotropy value of 0.87 confirms that there is significant coupling between the temperature compo-

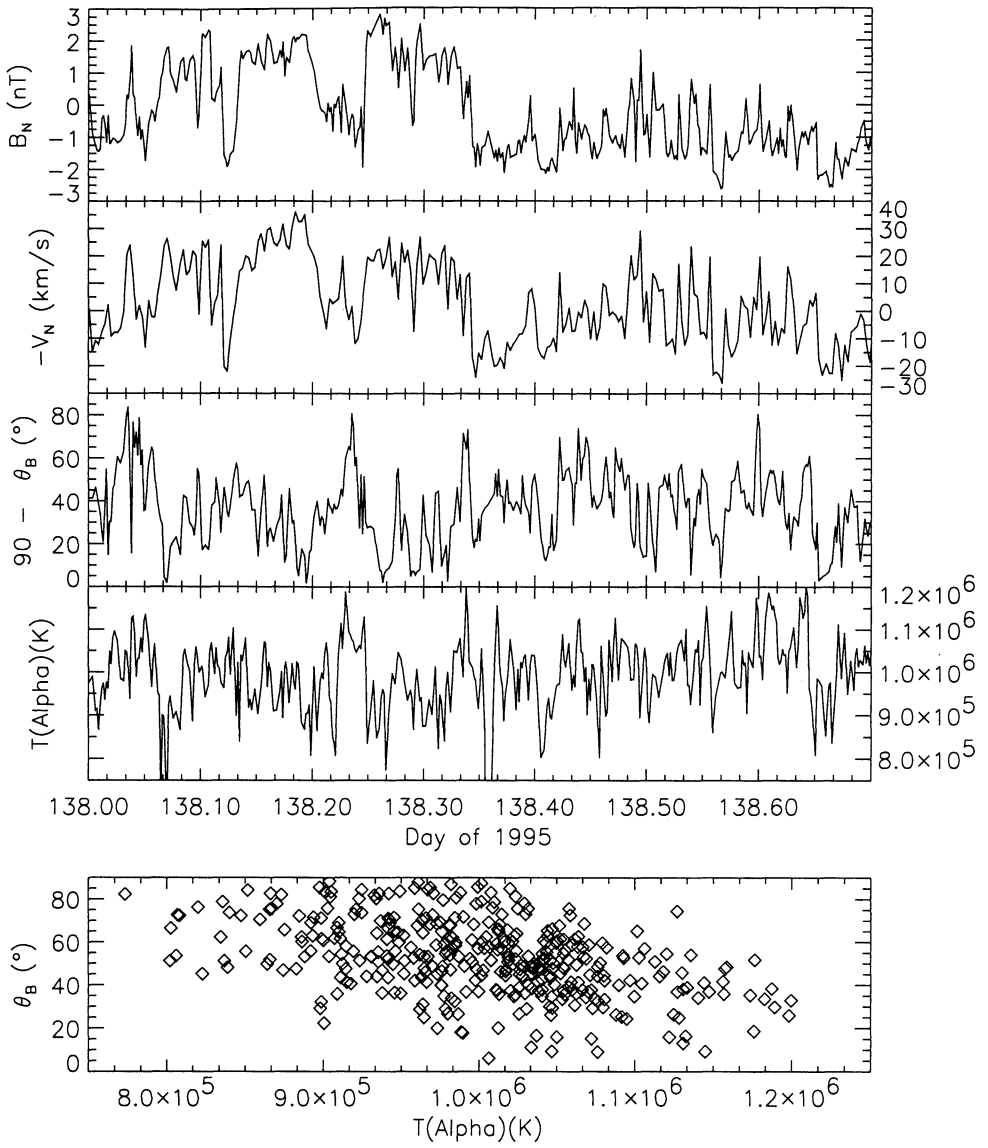

Figure 3. Correlation of radial temperature fluctuations with Alfvén waves. Top two panels plot the N-S magnetic field component B_N and velocity component v_N, respectively, for a typical 16-hour period in the high-latitude wind ($\lambda = 53.6°, r = 1.53$ AU). The strong degree of (anti)correlation seen between these two components demonstrates that the B field fluctuations are almost purely Alfvénic. Next two panels plot θ_B, the angle of B with respect to the radial (antisunward) direction, and T_α, the alpha particle temperature, respectively. A weak (anti)correlation is observed. The anticorrelation is more apparent in the bottom panel, a scatterplot of θ_B versus T_α. The temperature change as the field rotates is a consequence of a significant temperature anisotropy, $T_\perp/T_\parallel = 0.7$.

nents. Although the actual coupling mechanism is not known, we can nevertheless calculate an "effective" collision rate $\nu_{\text{eff}}(r)$ necessary to drive the temperature components to near isotropy. In Appendix A, we calculate $\nu_{\text{eff}}(r)$ with the assumption of a Parker spiral magnetic field configuration. The resulting relation for the effective collision frequency (equation (A10)) can be easily evaluated as a function of the proton speed, the heliographic latitude, and the solar rotation rate. This can be compared to the average alpha-proton Coulomb collision frequency and the proton cyclotron frequency ($\Omega_p = B/65.8$, where B is in nanoteslas). The $\nu_{\text{eff}}(r)$ and the cyclotron frequency can readily be calculated from the Ulysses data. The alpha-proton collision frequency for relaxation of the temperature anisotropy was originally derived by *Kogan* [1961] and can be found in the Naval Research Laboratory (NRL) Plasma Formulary [*Book*, 1998]. All these frequencies are plotted versus heliocentric distance in Figure 5 between 1.5 and 4.5 AU. The effective collision frequency is calculated from (A10) assuming a constant proton velocity of 767 km s^{-1}, the average solar wind speed for the northern polar

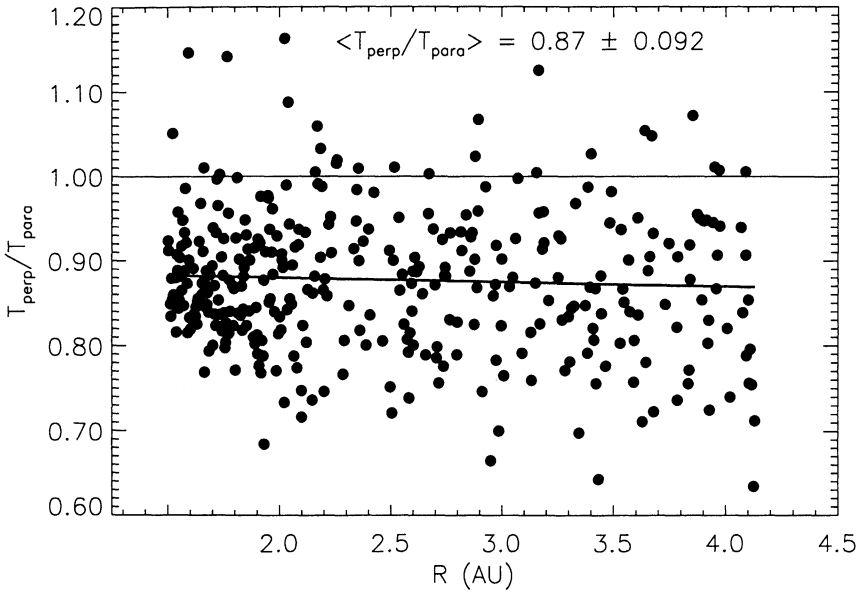

Figure 4. Dependence of the alpha temperature anisotropy $T_\perp/T_\parallel$ on heliocentric distance. See text for description of method for calculating temperature anisotropy. Each point represents the ratio for a single 12-hour period.

pass [*McComas et al.*, 2000]. It can be seen that $\nu_{\rm eff}(r)$ is ~4 orders of magnitude larger than the Coulomb collision frequency, reconfirming that Coulomb collisions are not a likely mechanism for isotropizing the plasma. The relaxation time corresponding to $\nu_{\rm eff}(r)$ is $\sim 10^5$ s, which is roughly 10^3 times the cyclotron period. Recent simulations of the electromagnetic proton cyclotron anisotropy instability [*Gary et al.*, 2000c] yield proton anisotropy reduction frequencies ν_p in the range $10^{-3} \leq \nu_p/\Omega_p \leq 0.10$, indicating that ion-driven electromagnetic instabilities are capable of yielding the observed $\nu_{\rm eff}$. We suggest that this anisotropy reduction rate can serve as a useful constraint on any wave-particle or other scattering theory which attempts to describe the observed alpha temperature anisotropy. We will return to this issue in the discussion.

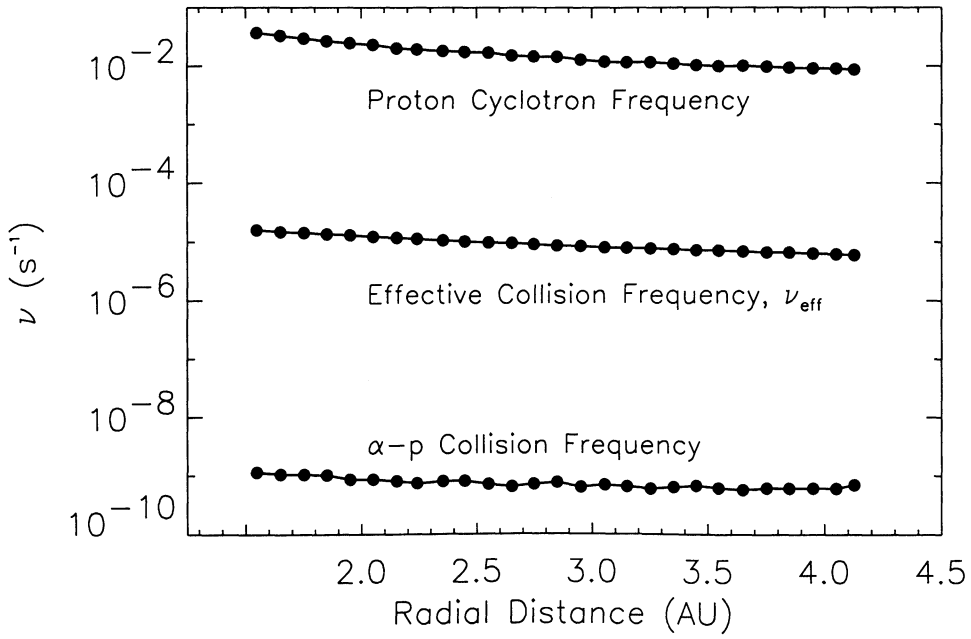

Figure 5. Various derived timescales as a function of heliocentric distance. Top curve shows proton cyclotron frequency, middle curve shows effective collision frequency needed to account for observed temperature anisotropy, and bottom curve shows alpha-proton Coulomb collision frequency.

It is worth noting that *Marsch and Richter* [1987] follow a procedure similar to the one described here to derive an effective collision frequency for the proton temperature isotropization based on the proton temperature anisotropy observed by Helios. They report an anisotropy of 0.9 that is nearly constant between 0.3 and 1.0 AU and nearly independent of flow speed. It is coincidental that the Helios proton anisotropy is nearly equal to the Ulysses alpha anisotropy, but given that the calculation only depends on the degree of anisotropy and not the ion species, it should be no surprise that the resultant collision frequency they derive has the same magnitude and radial dependence as what we report here.

We also consider the implications of the observed weak anisotropy on the assumption made in the previous section that the expected radial temperature dependence for adiabatic expansion is $r^{-4/3}$. Since this is only true for an isotropic plasma, we should evaluate what the expected adiabatic radial falloff in temperature is for slightly anisotropic plasma. As the anisotropy is roughly constant with distance, our job is greatly simplified since we know that $T_{\|\alpha}$ and $T_{\perp\alpha}$ will have the same radial functional dependence. In Appendix A we calculate the radial temperature dependence for adiabatic expansion of a nonisotropic, magnetized plasma (A9). Assuming an alpha temperature anisotropy of 0.87 and again using a proton velocity of 767 km s^{-1}, $T(r)_\alpha$ is well approximated between 1 and 5 AU by a power law:

$$T(r)_\alpha \propto r^{-1.28}. \tag{4}$$

The observed fluctuation of the solar wind speed is only ± 24 km s^{-1}, which adds negligible uncertainty. The latitude dependence of $T(r)_\alpha$ for latitudes between 30° and 80° is also negligible. The difference between this gradient and the $r^{-4/3}$ dependence of an isotropic plasma is quite small, particularly as compared to the observed $r^{-0.80}$ dependence of the alpha temperature. Thus our conclusion that the alpha particles experience excess heating stands.

3.3. Radial Evolution of Helium Energetics

Now we turn to an analysis of the energetics of the helium streaming. Ulysses observations of the high-latitude alpha-proton differential speed from the first orbit northern polar pass are presented in Figure 6a. The average $v_{\alpha p}$ starts at ~40 km s^{-1} at 1.5 AU and smoothly slows to ~15 km s^{-1} by 4.1 AU. In Figure 7 we compare the steadily decreasing free energy available in the alpha streaming to the non-adiabatic heat content of the alpha particles as a function of heliocentric distance. The alpha free energy is simply calculated as $K(r) = 1/2 m_\alpha v_{\alpha p}^2(r)$. As discussed in section 3.1, the alphas are at a temperature above that expected for adiabatic expansion. We can estimate the required heat input $Q(r)$ by calculating

$$Q(r) = \frac{3}{2} k T(r) - \frac{3}{2} k T_0 r^{\frac{4}{3}}, \tag{5}$$

where T_0 is a normalization constant such that for $R = 1.5$ AU, the closest distance of the Ulysses spacecraft to the Sun for our data set, $Q = 0$. That is, $T_0 = T(R = 1.5)/(1.5)^{-4/3}$. Each point in Figure 7 represents an average of these parameters over 0.1 AU bins.

The sum of the two quantities $K(r)$ and $Q(r)$ is also plotted in Figure 7. This sum is essentially constant with radius, having a mean value of $4.47 \pm 0.43 \times 10^{11}$ ergs. This suggests that the energy liberated as the alphas decelerate acts to heat the alpha particles. We consider this a very significant result, as it is highly unlikely that these two quantities would coincidentally balance.

The balance is perhaps all the more remarkable because we are not following the evolution of individual flux tubes. Rather, we sample the plasma of many flux tubes that have different histories, as governed by the properties of their foot points in the photosphere. Furthermore, there are weak stream interactions at high latitudes (coined "microstreams" by *Neugebauer et al.* [1995]) that generate small (~±25%) temperature fluctuations. Regardless of source, any temperature fluctuations are amplified in the sum $K(r) + Q(r)$, because $Q(r)$ is defined in terms of a temperature difference. At small distances the variation of $K(r)+Q(r)$ is most pronounced because the difference $T(r) - T_0 r^{4/3}$ is small, less than ~10% of $T(r)$. By 4 AU the difference has grown to ~ 60% of $T(r)$, and the fluctuations are significantly diminished.

In the Introduction we mention the potential ability of "rotational" forces to slow the alphas. As the alpha particles are turned by the tightening Parker spiral, they experience a centripetal force which slows them at the expense of accelerating the protons. Because of the looser winding of the magnetic field at higher latitudes, alphas at higher latitudes should experience a much smaller rotational force. In Figure 8 we compare the $v_{\alpha p}$ radial profile observed by Ulysses to that expected by sole action of the rotational force. We also compare the high-speed wind $v_{\alpha p}$ profile observed by Helios between 0.3 and 1.0 AU [*Marsch et al.,* 1982a] to the Helios profile expected because of the rotational force. Our calculation follows from the derivation of *McKenzie et al.* [1979]. For the Ulysses calculated profile we take 150 km s^{-1} as the initial differential speed at 0.3 AU, reflecting the Helios high-speed wind observations.

For this calculation we have assumed a "classic" Parker spiral, reflecting the field configuration based on the assumption that the Sun is a perfect monopole. The observed interplanetary magnetic field at solar minimum is under-wound compared to the classic Parker spiral as a consequence of the overexpansion of the polar coronal holes [*Smith et al.*, 1997]. The analytic solar magnetic field model of *Banaszkiewicz et al.* [1998], which reproduces these observations, describes a spiral field that is under-wound by 20% at the equatorial current sheet, 10% under-wound at a latitude of 60°, and

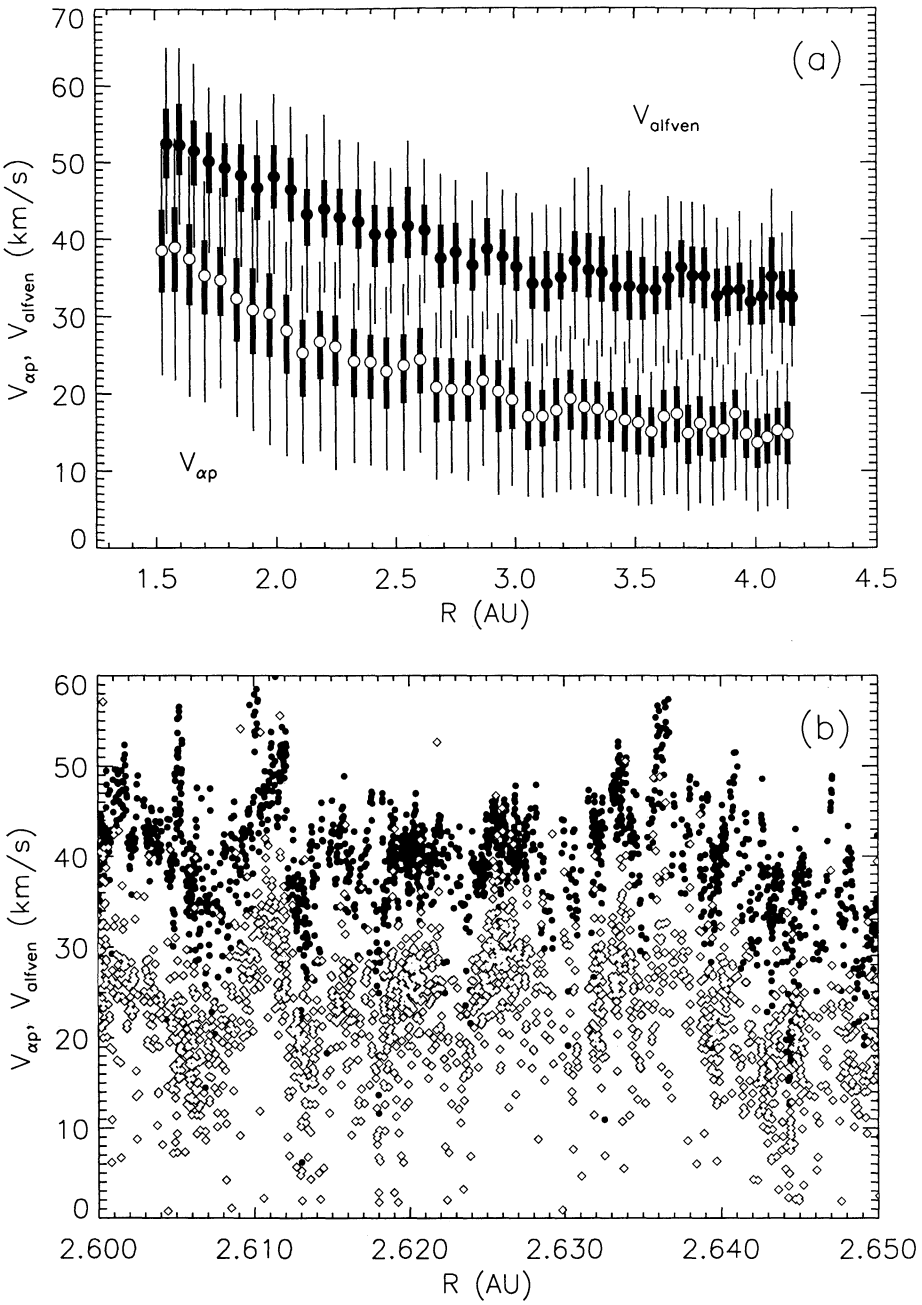

Figure 6. (a) Differential alpha-proton streaming velocity magnitude $v_{\alpha p}$ (solid circles), and the Alfvén speed v_A (open circles) as a function of heliocentric distance. Each bar characterizes the speed distributions over 10-day bins, as described in Figure 1. Note that not only do both $v_{\alpha p}$ and v_A decrease with radial distance, but also $v_{\alpha p}$ appears to track the small-scale fluctuations ($\sim$ 0.1 AU) in the radial evolution of v_A. (b) Same as Figure 6a, except over a much narrower range of distance, showing that on even smaller scales, $v_{\alpha p}$ (solid circles) tracks v_A (grey diamonds).

"correctly" wound over the poles. The rotational forces due to such a field would be even smaller than those described here; thus our calculation can be considered a worst case.

From Figure 8 we conclude that the rotational force alone cannot explain the observed $v_{\alpha p}$ profiles. In fact, the predicted profiles have the wrong shapes. When Ulysses is near 80° (2 AU), the field is essentially radial and there is negligible deceleration due to rotation. Hence at 2 AU the predicted Ulysses $v_{\alpha p}$ observation is actually faster than at 1.5 AU (where Ulysses was at ~45°). The Ulysses data show no evidence of this; rather, the observed profile is, in fact, most rapidly decreasing across this range. The discrepancy between Helios predicted and observed $v_{\alpha p}$ is even greater. Thus the observations imply that the rotational force has little effect on the differential streaming deceleration.

By contrast, the observed quasiconservation of $K(r)+Q(r)$ shown in Figure 7 suggests that a local mechanism capable of transferring heat to the alphas must be in ac-

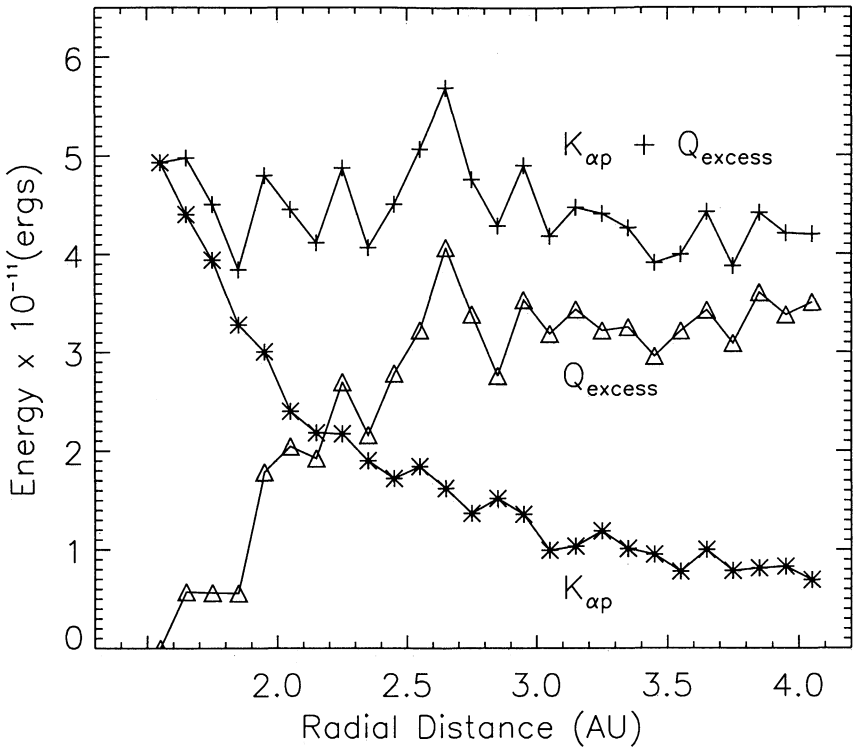

Figure 7. Alpha particle energy balance as a function of heliocentric distance. Asterisks indicate the excess heat present in the alphas relative to their expected heat content assuming adiabatic expansion. Triangles represent the free energy available in the differential streaming. Crosses indicate the sum of these two quantities. The rough conservation of the sum as a function of distance suggests the conversion of streaming energy into alpha heating as the alpha-proton streaming speed decreases.

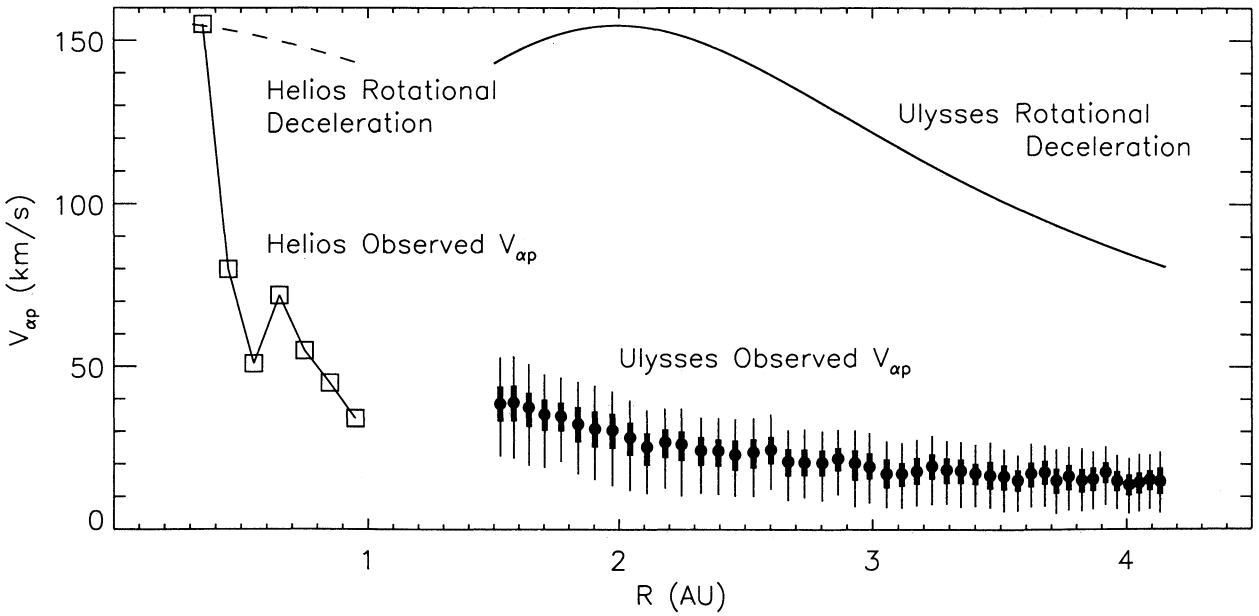

Figure 8. Comparison of the radial dependence of $v_{\alpha p}$ observed by Ulysses (solid bars) and the $v_{\alpha p}$ Ulysses would be predicted to observe were the $v_{\alpha p}$ deceleration due to solely the action of the "rotational" force (solid curve). For Ulysses observations, thin bars span the 5-95% percentiles and the thick bars span the 25-75% percentiles. For predicted $v_{\alpha p}$ it is assumed $v_{\alpha p}$ = 150 km s^{-1} at 0.3 AU (based on Helios observations [*Marsch et al.*, 1982a]). Also shown is $v_{\alpha p}$ observed by Helios for high-speed wind (700-800 km s^{-1}) between 0.3 and 1 AU (squares). Again for comparison, we show the predicted $v_{\alpha p}$ that Helios would observe were the deceleration due to only the rotational force (dashed curve).

tion, such as the magnetosonic instability suggested by *Gary et al.* [2000b] and discussed further in section 4. Stated another way, the observed balance between $K(r)$ and $Q(r)$ places a clear constraint on any theory attempting to explain the deceleration of the alphas: any such theory must predict the transfer of the dissipated streaming energy into the ultimate heating of the alpha particles.

3.4. Differential Streaming

A further clue to aid our understanding of the mechanism governing the $v_{\alpha p}$ deceleration may lie in the relationship between the alpha-proton differential speed and the Alfvén speed. Ulysses observations of alpha-proton differential streaming at high latitudes have been reported by *Neugebauer et al.* [1996], who show the gradual decrease in the ratio $v_{\alpha p}/v_A$ with heliocentric distance. Here we expand on their work and compare $v_{\alpha p}$ to the local Alfvén speed in more detail. Figure 6a plots the average for both $v_{\alpha p}$ and v_A over 0.1 AU bins as a function of radial distance. What stands out foremost is that $v_{\alpha p}$ is lower than v_A, dropping from ~80% of the Alfvén speed at 1.5 AU to ~45% at 4.2 AU. Although the fractional difference grows, the relative speed difference between $v_{\alpha p}$ and v_A remains a relatively constant 15 km s^{-1}. The second point to notice is that $v_{\alpha p}$ roughly tracks v_A, as can be seen by the obvious correlation between the fluctuations in $v_{\alpha p}$ and in v_A. Figure 6b, which plots $v_{\alpha p}$ and v_A between 2.60 and 2.65 AU, shows that on even very short distance scales (0.05 AU), $v_{\alpha p}$ tracks v_A. (The gaps in the time series shown in Figure 6b are due to the selection criterion in the calculation of $v_{\alpha p}$ that the cosine of the angle between the magnetic field and the radial direction be >0.3. As discussed in section 2, we do this to limit the instrumental uncertainly in the determination of $v_{\alpha p}$.)

The implication of the spatial correlation between $v_{\alpha p}$ and v_A is that v_A somehow governs the differential streaming. Such would be the case if, for example, $v_{\alpha p}$ is limited by the magnetosonic instability (see section 4 and *Gary et al.* [2000b]). However, theory suggests the instabilities usually act only when $v_{\alpha p} \gtrsim v_A$, which is clearly not the case here. Nevertheless, the tracking of $v_{\alpha p}$ with v_A still implies a mechanism must be at work to slow $v_{\alpha p}$, which likely involves an electromagnetic instability.

That $v_{\alpha p}$ rarely exceeds the local Alfvén speed may, in fact, not be a problem for the proposed theoretical mechanisms. Again turning to Figure 6a, we notice that within a given 0.1 AU bin, the maximum values of $v_{\alpha p}$ approach but rarely exceed the minimum value of v_A. Because the alpha particles are streaming through the proton population (which, along with B, largely determine the Alfvén speed), this suggests that at some point in a given alpha particle's past, its differential speed did reach and possibly exceed the local Alfvén speed. If this occurs, then the conditions for instability are met, possibly causing the particle to slow rapidly to the observed situation of $v_{\alpha p} < v_A$. We will return to this point later in section 4, where we discuss a possible instability mechanism that may operate in this regime. We note that a similar argument is used by *Goldstein et al.* [2000] in the context of proton-proton differential streaming to explain why the bulk of the observed proton-proton speed differences are considerably below the threshold for their proposed instability-driven damping mechanism.

We can, in fact, estimate the frequency with which alpha particles drifting through the proton flow will encounter regions where $v_{\alpha p}/v_A \gtrsim 1$. The procedure we follow is based on the premise that the time series of plasma observations taken by Ulysses can be converted into a spatial map of the solar wind. That is, if the variations in the time series solar wind measurements are due to spatial variations propagating past the spacecraft, then Ulysses measurements at earlier times can be used to project the solar wind parameters to spatial locations beyond Ulysses for later times. Because the alphas stream relative to the protons along field lines, ideally, we require a map of plasma variations along a flux tube. However, we do not have such data; the time series observations are not samples along any single flux tube but, instead, are samples of plasma from many adjacent flux tubes convecting past the satellite. We have no choice but to use our derived spatial map as a proxy for the plasma environment the alpha particles would experience as they flow along a flux tube. Since we are only interested in obtaining the order of magnitude of the drift time, we believe that our proxy approach is reasonable.

We construct the spatial map from the time series measurements by the following procedure. For each point in the time series, we determine a time $t_{\rm stream}$, the estimated time for an alpha particle to propagate into a region of instability. Given a sample at time $t = t_0$, we take the local value of the alpha-proton drift speed $v_{\alpha p}(t_0)$ and then march backward through the time series until we reach a time t^* where the condition $v_{\alpha p}(t_0)/v_A(t^*) \geq 1$ is met. That is, by marching back to earlier times we are approximating a look at solar wind conditions farther out than Ulysses is at time t_0. Presumably, when the above condition is met, the alpha beam becomes unstable and will then slow down. The time interval in the spacecraft time series $(t^* - t_0)$ can then be converted into the time $t_{\rm stream}$ that the alpha population located at $r(t_0)$ takes to drift into the region where the beam becomes unstable:

$$t_{\rm stream} = \frac{(t^* - t_0)\langle v_p - v_r^{sc}\rangle}{v_{\alpha p}(t_0)\langle \cos\phi_B\rangle}, \qquad (6)$$

where v_r^{sc} is the radial component of the spacecraft velocity and $\langle \cos\phi_B\rangle$ is the cosine of the Parker spiral angle averaged over the range $[r(t_0), r(t^*)]$. Including $\langle \cos\phi_B\rangle$ corrects for the fact that the alphas drift along the field rather than radially. Note, however, that we

make no attempt to account for fluctuations in the magnetic field, such as from Alfvén waves.

If the distance the solar wind travels in this time is a significant fraction of an astronomical unit, then the Alfvén speed observed by the spacecraft must be adjusted to take into account the $r^{-0.5}$ falloff of v_A that occurs in the high-latitude solar wind [*McComas et al.*, 2000]. Then our instability criteria in the solar wind downstream of the spacecraft becomes

$$\frac{v_{\alpha p}(t_0)}{v_A(t^*)}\left[\frac{r(t^*)}{r(t^*)+\frac{(t^*-t_0)v_p\langle v_p-v_r^{sc}\rangle}{v_{\alpha p}(t_0)\langle\cos\phi_B\rangle}}\right]^{1/2} \geq 1. \quad (7)$$

We are only concerned with that part of the alpha population that requires slowing by the time it reaches 4.2 AU. In Figure 6 we see that the median of $v_{\alpha p}$ approaches a value of $\sim$ 15 km s^{-1} by 4.2 AU, with the bulk of the alphas within $\pm$ 3 km s^{-1}of this mark. Thus, the observations suggest that there is no requirement that the alpha population flowing at or below $\sim$18 km s^{-1} need ever become unstable to a beam instability. In fact, including this population would incorrectly skew the average streaming time to longer times because it is so infrequent that $v_A \lesssim 18$ km s^{-1} (until well beyond 4 AU). We therefore include in our analysis only differential speeds observed for which $v_{\alpha p} \geq 18$ km s^{-1}.

The resulting streaming times are presented in Figure 9 as a function of initial alpha observation location (solid circles). The curve drawn through the points represents a best fit to the data, having the form $t_{\rm stream} = 1.49r^{1.47}$, where $t_{\rm stream}$ is given in days. The results are also represented in terms of the free streaming distance (right axis of graph) determined by scaling the streaming time by the average high-latitude flow speed, 767 km s^{-1}. We see that alphas streaming at 1.5 AU will stream, on average, $\sim$2.5 days (1 AU) before entering an instability region; by 3 AU the alphas will stream $\sim$6 days (2.75 AU) before entering an instability region. On the basis of this, we expect to see most of the beam deceleration between 1.5 and 3 AU, whereas beyond 3 AU, it is unlikely for the beam to decelerate much more before the alphas reach 4.2 AU, the limit of the high-latitude solar wind observation range. As we see in Figure 6, this is just what is observed to occur.

Once plasma enters an instability region, we can ask how much time is available for the instability to act before the critical condition $v_{\alpha p}/v_A \geq 1$ is no longer met. To address this, we have calculated the instability duration time in a manner similar to the calculation of the streaming time. This result is also presented in Figure 9 (open circles). Again, an empirical curve is fit to the data, of the form $t_{\rm instability} = 0.0839r^{1.94}$. Thus, for example, plasma observed at 1.5 AU will stream for $\sim$2.5 days and then enter an instability region lasting for, on average, 0.2 days. Note that the streaming and instability curves have roughly the same functional shape, and the ratio $t_{\rm instability}/t_{\rm stream}$ is, on average, $\sim$0.085 (the range is 0.07 at 1.5 AU to 0.10 at 4.2 AU). Thus

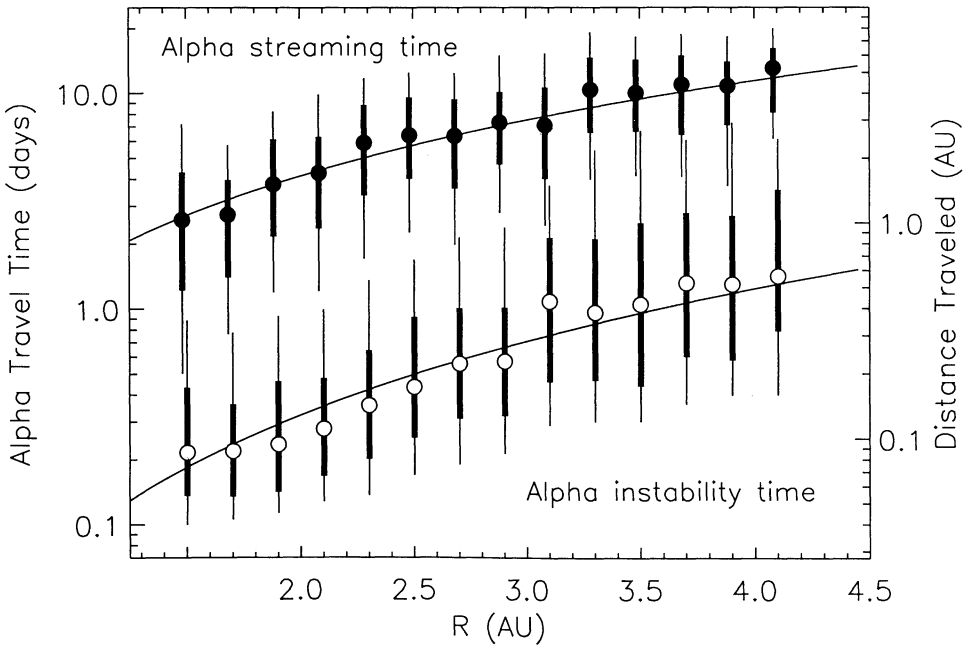

Figure 9. Average time for alpha particles to drift into region where the instability condition $v_{\alpha p}/v_A \geq 1$ is met as a function of heliocentric distance (solid circles) and average time duration alpha particles spend in instability region (open circles). Thin bars span the 5-95% percentiles, and the thick bars span the 25-75% percentiles. Distance alphas travel in these times is indicated by scale on right-hand axis, assuming a proton flow speed of 767 km s^{-1}. Curves drawn through the points represent best fits to the data.

the instability is in action for ~8.5% of the time the solar wind flows outward. We point out that the calculated instability duration time is an upper limit. We do not account for the effect of the instability, namely, the deceleration of the alpha beam. We are only working with empirical information and do not speculate on the strength of the instability action that slows down the beam. Thus it may be the case that the duration of the instability is shorter since the instability condition $v_{\alpha p}/v_A \geq 1$ may no longer be met after the instability mechanism has had some time to act.

4. Discussion

We have presented the following key observational results for alpha particles in the high-latitude solar wind: (1) Energy is deposited in the form of heat into the alpha particles as they stream outward. (2) The alpha-proton differential streaming velocity gradually decreases with distance from the Sun. (3) Helium ions exhibit a weak temperature anisotropy ($T_{\perp\alpha}/T_{\|\alpha} = 0.87$) that is constant with distance, on average. (4) The ratio of the streaming speed $v_{\alpha p}$ to the Alfvén speed v_A steadily drops from 0.80 at 1.5 AU to 0.45 at 4.2 AU; however, at all distances the maximum $v_{\alpha p}$ roughly matches the minimum v_A.

In addition, we have presented a set of derived results based on these solar wind observations: (5) We have calculated the nonadiabatic heat content of the alphas, arriving at the important result that this heat excess closely matches the amount of energy dissipated as the alpha-proton streaming decreases. (6) On the basis of the observed helium anisotropy, we have computed the collision rate necessary to counter the expected anisotropy growth with distance as is dictated by double-adiabatic invariance. The calculated collision frequency is $\sim 10^{-5}$ s^{-1}. (7) Finally, we have estimated the distance alphas must travel, on average, until they enter a region where the critical condition $v_{\alpha p}/v_A \geq 1$ is met, with the result that alphas observed between 1.5 and 3.0 AU should become unstable to the magnetosonic beam instability before reaching 4.2 AU, the boundary of the range covered by the Ulysses high-latitude observations. Furthermore, the size of the instability region is such that alphas will spend, on average, ~8.5 % of their time in such regions as they travel out to 4.2 AU.

The core issue that this study leaves unexplained is what actual physical mechanism (mechanisms) is (are) responsible for slowing and heating the alpha beam and maintaining the observed anisotropy. However, we believe this set of observations strongly constrains any theory that attempts to model the physics. Alpha/proton microinstability models have recently appeared in the literature that may serve as candidates [*Li and Habbal*, 2000; *Gary et al.*, 2000a].

Models based on wave-particle scattering have the potential to explain all of these observations. A plausible scenario is as follows: In the solar corona, wave-particle interactions accelerate helium ions (as well as all heavy ions) to speeds substantially greater than the average proton flow speed. As the solar wind expands away from the Sun, the Alfvén speed decreases so that eventually the alpha/proton relative flow speed exceeds the threshold condition of one or another kinetic instability. Excitation of these short-wavelength growing modes leads to enhanced electromagnetic fluctuations; the fluctuations, in turn, scatter the alphas. Various instabilities yield different consequences, but all alpha/proton instabilities yield two common results: the alpha/proton relative flow velocity is reduced, and the alphas are heated more strongly than the protons.

In this scenario, points (2) and (5) above are a natural consequence; wave-particle scattering translates relative kinetic energy into thermal energy. Whether or not points (3) and (4) are satisfied depends on which alpha/proton instability is excited; and satisfaction of point (1) may depend on the variation of a critical parameter, such as the proton beta β_p, with distance from the Sun, which may determine the relative heating rates of the alphas and the protons. In order to demonstrate the self-consistency of any model, it must finally be shown to operate at a frequency necessary to satisfy (6) and (7).

Hybrid simulations of the alpha/proton magnetosonic and Alfvén instabilities have recently been carried out [*Gary et al.*, 2000a, b]. If $v_{\alpha p}/v_A \simeq 1$, the latter modes have appreciable growth rates only at a proton parallel beta $\beta_{\|p} << 1$ [*Daughton and Gary*, 1998] and thus are unlikely to play an important role in scattering alphas in the high-speed solar wind (where $1 \lesssim \beta_{\|p} \lesssim 3$). However, Figure 4 clearly demonstrates $T_{\perp\alpha}/T_{\|\alpha} < 1$, and as *Li and Habbal* [2000] showed, this anisotropy reduces the value of $v_{\alpha p}/v_A$ necessary to excite the magnetosonic mode. *Gary et al.* [2000b] carried out hybrid simulations of the magnetosonic instability with initially anisotropic alphas. The simulations showed that wave-particle scattering by enhanced fluctuations from the alpha/proton magnetosonic instability yields an increase in T_α/T_p, a reduction in the alpha temperature anisotropy and, at $\beta_{\|p} > 2$, a decrease of the alpha/proton relative flow speed to $v_{\alpha p}/v_A \leq 1$.

Under the parameters used by *Gary et al.* [2000b], the magnetosonic instability cannot be excited or reduce the alpha/proton relative drift if $v_{\alpha p}/v_A \leq 1$ and $\beta_{\|p} \leq 2$. This may be a serious limitation on the application of this mode, because the relatively large values of $v_{\alpha p}/v_A$ used in the $\beta_{\|p} \leq 2$ simulations of *Gary et al.* [2000b] are not observed by Ulysses. However, we note that the magnetosonic instability threshold value of $v_{\alpha p}/v_A$ is diminished by a reduction in $T_{\perp\alpha}/T_{\|\alpha}$ [*Li and Habbal*, 2000]. A stronger anisotropy than the one reported here may, in fact, be present in the high-latitude solar wind. Recall the recipe we use for determining $T_{\perp\alpha}/T_{\|\alpha}$ averages of the anisotropy over 12-hour inter-

vals, which will have the effect of smoothing out any stronger anisotropies present at higher time resolution. So, if higher time resolution measurements of the alpha anisotropy could be made in the solar wind and if those measurements could show stronger alpha anisotropies than those reported above, the magnetosonic instability could become active at $v_{\alpha p}/v_A \simeq 1$ and $\beta_{\|p} \leq 2$, thereby corresponding to a greater share of the Ulysses observations.

Thus, at least in a qualitative sense, the alpha/proton magnetosonic instability has the capability to yield the following observed solar wind properties: (1) the alphas are heated, (2) the alpha/proton differential streaming velocity is reduced with distance from the Sun, and (3) the alphas maintain a weak temperature anisotropy $T_{\perp\alpha}/T_{\|\alpha} < 1$. So we believe that the simulations support, if not validate, the scenario described above and that the magnetosonic instability may play an important role in determining the properties of alpha particles in the solar wind.

To conclude, we return to the most intriguing observational aspect of the paper, namely, that the nonadiabatic heat content of the alphas matches the energy dissipated as the alpha-proton streaming speed decelerates (Figure 7). As there is no a priori relation between these two quantities, it is highly unlikely that they would necessarily balance. It appears therefore that this is a fundamental measurement of energy transfer from the kinetic flow to the internal motion of solar wind helium.

Appendix A: Radial Dependence of Solar Wind Temperature Components

In the absence of strong collisional coupling between the particle constituents in the solar wind, the particle distribution functions are not guaranteed to be isotropic as they are for an ideal gas. Thus expectations for the energetics of solar wind evolution may be flawed if they are based on the behavior of an ideal gas. Here we investigate the degree of departure of the alpha particles from ideal gas behavior based on the observed alpha temperature anisotropy.

We start with the double-adiabatic invariant relations (equations 2 and 3), and following *Phillips and Gosling* [1990], we reduce them to relations relating the alpha temperature components to the interplanetary magnetic field B and the heliocentric distance r. In the limit of time stationary evolution and purely radial outflow, $dt \rightarrow v_r dr$, and by conserving alpha flux, equations 2 and 3, become

$$\frac{dT_{\|}}{dr} = -T_{\|}\left(\frac{4}{r} + \frac{1}{B^2}\frac{d}{dr}B^2\right), \quad \text{(A1)}$$

$$\frac{dT_{\perp}}{dr} = \frac{T_{\perp}}{B}\frac{d}{dr}B. \quad \text{(A2)}$$

As the purpose here is to generate some basic intuition for the evolution of alpha distributions in the absence of strong coupling rather than performing a rigorous study, we make the simplifying assumption that the magnetic field can be described with a spiral model dependent on a constant convection speed v, solar rotation rate Ω, and heliographic latitude θ, in the usual manner. We can eliminate B from the above equations, arriving at

$$\frac{dT_{\|}}{dr} = -T_{\|}\frac{2r\Omega^2\cos^2\theta}{v^2 + \Omega^2\cos^2\theta r^2}, \quad \text{(A3)}$$

$$\frac{dT_{\perp}}{dr} = -T_{\perp}\frac{2v^2r^{-1} + \Omega^2\cos^2\theta r}{v^2 + \Omega^2\cos^2\theta r^2}. \quad \text{(A4)}$$

As discussed in section 3.2, on the basis of these relations alone, one finds that the temperature will be highly anisotropic for any reasonable values of v, Ω, and θ. At this point we need to introduce collision terms to reproduce the observed weak anisotropy. However, incorporating explicit expressions based on a formal theory describing the rearrangement of internal energy between the particles is beyond the present scope. Following the lead of *Marsch and Richter* [1987], we instead use a simple relaxation time approximation incorporating an effective mean collision frequency $\nu_{\text{eff}}(r)$ to represent isotropic scattering events due to particle-particle or, more likely, wave-particle interactions. We implement collisional relaxation according to the following expressions, which ensure the invariance of the total internal particle energy:

$$\left(\frac{dT_{\perp}}{dt}\right)_{\text{coll}} = -\frac{1}{2}\left(\frac{dT_{\|}}{dt}\right)_{\text{coll}} = \nu_{\text{eff}}(T_{\|} - T_{\perp}). \quad \text{(A5)}$$

On the basis of this expression, we now add additional terms to the right side of (A3) and (A4) to yield the following coupled equations:

$$\frac{dT_{\|}}{dr} = -T_{\|}\frac{2r\Omega^2\cos^2\theta}{v^2 + \Omega^2 cos^2\theta r^2} - \frac{2\nu_{\text{eff}}(T_{\|} - T_{\perp})}{v}, \quad \text{(A6)}$$

$$\frac{dT_{\perp}}{dr} = -T_{\perp}\frac{2v^2r^{-1} + r\Omega^2\cos^2\theta}{v^2 + r^2\Omega^2\cos^2\theta} + \frac{\nu_{\text{eff}}(T_{\|} - T_{\perp})}{v}. \quad \text{(A7)}$$

Phillips and Gosling [1990] replace ν_{eff} with an expression for the Coulomb collision rate in order to predict a temperature anisotropy for electrons. Here we use the observed alpha anisotropy and introduce it into (A6) and (A7) to determine $T_{\perp}(r)$, $T_{\|}(r)$, and $\nu_{\text{eff}}(r)$. Since the anisotropy $A \equiv T_{\perp}/T_{\|}$ is observed to be, on average, constant with radius, the calculation is greatly simplified. In fact, the solutions have an analytical form (again, v is considered a constant here):

$$T_\perp(r) = AT_\parallel(r), \quad \text{(A8)}$$

$$T_\parallel(r) = T_{\parallel 0} r^{-2C} \times (v^2 + r^2\Omega^2 \cos^2\theta)^{\frac{1}{2}(-2+3C)}, \quad \text{(A9)}$$

$$\nu_{\text{eff}}(r) = \left[\frac{1-A}{Av} + \frac{2(1-A)}{v}\right]^{-1} \times \left(\frac{2v^2 r^{-1} - r\Omega^2 \cos^2\theta}{v^2 - r^2\Omega^2 \cos^2\theta}\right), \quad \text{(A10)}$$

where $C = 2A/1 + 2A$. Note that in the limit $A \to 1$, $T_\parallel(r) \to T_{\parallel 0} r^{-4/3}$. The implications of these equations are addressed in section 3.2.

Acknowledgments. The authors wish to thank Bill Feldman for invaluable discussion at the beginning of this project. We would also like to thank John Dorelli and Lin Yin for their help. In addition, the authors greatly appreciate the careful reviews and helpful comments of the referees. This work was performed under the auspices of the U.S. Department of Energy with support from NASA's Ulysses program.

Janet G. Luhmann thanks Robert F. Wimmer-Schweingruber and another referee for their assistance in evaluating this paper.

References

Asbridge, J. R., S. J. Bame, W. C. Feldman, and M. D. Montgomery, Helium and hydrogen velocity differences in the solar wind, *J. Geophys. Res., 81,* 2719, 1976.

Axford, W. I., J. F. McKenzie, G. V. Sukhorukova, M. Banaszkiewicz, A. Czechowski, and R. Ratkiewicz, Acceleration of the high-speed solar wind in coronal holes, *Space Sci. Rev., 87,* 25, 1999.

Balogh, A., et al., The magnetic field investigation on the Ulysses mission: Instrumentation and preliminary scientific results, *Astron. Astrophys. Suppl. Ser., 92,* 221, 1992.

Bame, S.J., et al., The Ulysses solar wind plasma experiment, *Astron. Astrophys. Suppl. Ser., 92,* 237, 1992.

Banaszkiewicz, M., W. I. Axford, and J. F. McKenzie, An analytic solar magnetic field model, *Astron. Astrophys., 337,* 940, 1998.

Book, D. L., *NRL Plasma Formulary,* p. 33, Nav. Res. Lab., Washington, D.C., 1998.

Borrini, G., J. T. Gosling, S. J. Bame, W. C. Feldman, and J. M. Wilcox, Solar wind helium and hydrogen structure near the heliospheric current sheet: A signal of coronal streamers at 1 AU, *J. Geophys. Res., 86,* 4565, 1981.

Chew, G. F., M. L. Goldberger, and F. E. Low, The Boltzmann equation and the one-fluid hydromagnetic equations in the absence of particle collisions, *Proc. R. Soc. London, Ser. A, 236,* 112, 1956.

Cranmer, S. R., G. B. Field, and J. L. Kohl, Spectroscopic constraints on models of ion cyclotron resonance heating in the polar solar corona and high-speed solar wind, *Astrophys. J., 518,* 937, 1999.

Daughton, W., and S. P. Gary, Electromagnetic proton/proton instabilities in the solar wind, *J. Geophys. Res., 103,* 20,613, 1998.

Daughton, W., S. P. Gary, and D. Winske, Electromagnetic proton/proton instabilities in the solar wind: Simulations, *J. Geophys. Res., 104,* 4657, 1999.

Feldman, W. C., J. R. Asbridge, S. J. Bame, and J. T. Gosling, Plasma and magnetic fields from the Sun, in *The Solar Output and Its Variation,* edited by O. R. White, p. 351, Colo. Assoc. Univ. Press, Boulder, 1977.

Feldman, W. C., B. L. Barraclough, J. T. Gosling, D. J. McComas, and P. Riley, Ion energy equation for the high-speed solar wind: Ulysses observations, *J. Geophys. Res., 103,* 14,547, 1998.

Gary, S. P., L. Yin, D. Winske, and D. B. Reisenfeld, Electromagnetic alpha/proton instabilities in the solar wind, *Geophys. Res. Lett., 27,* 1355, 2000a.

Gary, S. P., L. Yin, D. Winske, and D. B. Reisenfeld, Alpha/proton magnetosonic instability in the solar wind, *J. Geophys. Res., 105,* 20,989, 2000b.

Gary, S. P., L. Yin, and D. Winske, Electromagnetic proton cyclotron anisotropy instability: Wave-particle scattering rate, *Geophys. Res. Lett., 27,* 2,457, 2000c.

Goldstein, B. E., M. Neugebauer, L. D. Zhang, and S. P. Gary, Observed constraint on proton-proton relative velocities in the solar wind, *Geophys. Res. Lett., 27,* 53, 2000.

Gosling, J. T., Corotating and transient solar wind flow in three dimensions, *Annu. Rev. Astron. Astrophys., 34,* 35, 1996.

Gosling, J. T., On the determination of electron polytrope indices within coronal mass ejections in the solar wind, *J. Geophys. Res., 104,* 19,851, 1999.

Hefti, S., *et al.*, Kinetic properties of solar wind minor ions and protons measured with SOHO/CELIAS, *J. Geophys. Res., 103,* 29,697, 1998.

Hollweg, J. V., and P. A. Isenberg, On rotational forces in the solar wind, *J. Geophys. Res., 86,* 11,463, 1981.

Hollweg, J. V., and J. M. Turner, Acceleration of solar wind He^{2+}, 3, Effects of resonant and nonresonant interactions with transverse waves, *J. Geophys. Res., 83,* 97, 1978.

Kellogg, P. J., Fluctuations and ion isotropy in the solar wind, *Astrophys. J., 528,* 480, 2000.

Kogan, V. I., The rate of equalization of the temperatures of charged particles in a plasma, in *Plasma Physics and the Problem of Controlled Thermonuclear Reactions,* Engl. Trans., vol. 1, p. 153, Pergamon, Tarrytown, N.Y., 1961.

Kohl, J. L., et al., UVCS/SOHO empirical determinations of anisotropic velocity distributions in the solar corona, *Astrophys. J. Lett., 501,* L127, 1998.

Li, X., and S. R. Habbal, Proton/alpha magnetosonic instability in the fast solar wind, *J. Geophys. Res., 105,* 7483, 2000.

Marsch, E., and S. Livi, Observational evidence for marginal stability of solar wind ion beams, *J. Geophys. Res., 92,* 7263, 1987.

Marsch, E., and A. K. Richter, On the equation of state and collision time for a multicomponent, anisotropic solar wind, *Ann. Geophys., Ser. A, 5,* 71, 1987.

Marsch, E., K.-H. Mühlhäuser, H. Rosenbauer, R. Schwenn, and F. M. Neubauer, Solar wind helium ions: Observations of the Helios solar probes between 0.3 and 1 AU, *J. Geophys. Res., 87,* 35, 1982a.

Marsch, E., C. K. Goertz, and A. K. Richter, Wave heating and acceleration of solar wind ions by cyclotron resonance, *J. Geophys. Res., 87,* 5030, 1982b.

McComas, D. J., B. L. Barraclough, H. O. Funsten, J. T. Gosling, E. Santiago-Munoz, R. M. Skoug, B. E. Goldstein, M. Neugebauer, P. Riley, and A. Balogh, Solar wind observations over Ulysses' first full polar orbit, *J. Geophys. Res., 105,* 10,419, 2000.

McKenzie, J. F., and W. I. Axford, Comment on "On rotational forces in the solar wind" by J. V. Hollweg and P. A. Isenberg, *J. Geophys. Res., 88,* 7251, 1983.

McKenzie, J. F., W. H. Ip, and W. I. Axford, The acceleration of minor ion species in the solar wind, *Astrophys. Space Sci., 64,* 183, 1979.

Meister, C.-V., Anomalous diffusion in solar wind plasmas caused by electrostatic turbulence, in *Solar Wind Seven,* edited by E Marsch and R. Schwenn, p. 517, Max-Plank-Inst. für Aeron., Katlenburg-Lindau, Germany, 1992.

Neugebauer, M., Observations of solar-wind helium, *Fundam. of Cosmic Phys., 7,* 131, 1981.

Neugebauer, M., et al., Ulysses observations of microstreams in the solar wind from coronal holes, *J. Geophys. Res., 100,* 23,389, 1995.

Neugebauer, M., B. E. Goldstein, E. J. Smith, and W. C. Feldman, Ulysses observations of differential alpha-proton streaming in the solar wind, *J. Geophys. Res., 101,* 17,047, 1996.

Phillips, J. L., and J. T. Gosling, Radial evolution of solar wind thermal electron distributions due to expansion and collisions, *J. Geophys. Res., 95,* 4217, 1990.

Robbins, D. E., A. J. Hundhausen, and S. J. Bame, Helium in the solar wind, *J. Geophys. Res., 75,* 1178, 1970.

Schwenn, R., M.-H. Muhlhauser, E. Marsch, and H. Rosenbauer, Two states of the solar wind at the time of soar activity minimum, II, Radial gradients of plasma parameters in fast and slow streams, in *Solar Wind Four,* edited by H Rosenbauer, p. 126, Max-Plank-Inst. für Aeron., Katlenburg-Lindau, Germany, 1981.

Skoug, R. M., W. C. Feldman, J. T. Gosling, D. J. McComas, D. B. Reisenfeld, C. W. Smith, R. P. Lepping, and A. Balogh, Radial variation of solar wind electrons inside a magnetic cloud observed at 1 and 5 AU, *J. Geophys. Res., 105,* 27,269, 2000.

Smith, E. J., A. Balogh, M. Neugebauer, and D. J. McComas, Ulysses observations of Alfvén waves in the southern and northern solar hemispheres, *Geophys. Res. Lett., 22,* 3381, 1995.

Smith, E. J., A. Balogh, M. E. Burton, R. Forsyth, and R. P. Lepping, Radial and azimuthal components of the heliospheric magnetic field: Ulysses observations, *Adv. Space Res., 20*(1), 47, 1997.

Steinberg, J. T., A. J. Lazarus, K. W. Ogilvie, R. Lepping, and J. Byrnes, Differential flow between solar wind protons and alpha particles: First WIND observations, *Geophys. Res. Lett., 23,* 1183, 1996.

von Steiger, R., J. Geiss, G. Gloeckler, and A. B. Galvin, Kinetic properties of heavy ions in the solar wind from SWICS/Ulysses, *Space Sci. Rev., 72,* 71, 1995.

S. P. Gary, J. T. Gosling, D. B. Reisenfeld, and J. T. Steinberg, Space and Atmospheric Sciences, Los Alamos National Laboratory, MS D466 Los Alamos, NM 87545. (pgary@lanl.gov; jgosling@lanl.gov; dreisen@lanl.gov; jsteinberg@lanl.gov)

D. J. McComas, Instrumentation and Space Research Division, Southwest Research Institute P.O. Drawer 28510 San Antonio, TX 78228-0510. (dmccomas@swri.gov)

B. E. Goldstein and M. Neugebauer, Jet Propulsion Laboratory, MS 169-506, 2400 Oak Grove Pasadena, CA 91109. (bgoldstein@jplsp.jpl.nasa.gov; mneugeb@jplsp.jpl.nasa.gov)

(Received August 17, 2000; revised October 18, 2000; accepted October 26, 2000.)